Preparation and characterization of highly porous PVDF nanofibers and yarns

Taras Andrukh, Chip Few, Oleksandr Burtovyy, Ruslan Burtovyy, Igor Luzinov and Konstantin G.Kornev

School of Materials Science and Engineering,
Clemson University, 161 Sirrine Hall, Clemson, SC 29634-0971, kkornev@clemson.edu

ABSTRACT

Unique highly porous polyvinylidene difluoride (PVDF) nanofibers of about 50-500 nm in diameter were prepared by electrospinning. Electrospinning setup used allows controlling the nanofiber's placement on the gap-type electrodes. Nanofiber arrays and yarns can be freely suspended in the gap between the electrodes. The resulting nanofiber samples are uniform and do not require expensive purification. Electrospun nanofiber yarns are waterproof. Water drop deposited on the yarn's surface does not penetrate into the bulk. The PVDF yarns have high tenacity, can be bent, knotted, or twisted without any breakage. Results of DSC, TGA, and FTIR characterization of the yarns show the presents of crystalline PVDF β-phase responsible for ferroelectric properties of the PVDF material. Porosity of electrospun nanofibers was determined using SEM and AFM.

1 INTRODUCTION

Nanofibers have gained tremendous attention in research field of science and technology. Incorporating electronic devices into clothing is an important area of research geared toward manufacturing of multifunctional garments for broad applications (1). Soldier uniforms, sport and medical textiles are just a few potential targets. In this paper, we describe electrospun nanofiber yarns, which are expected to form a new class of fiber-based materials for wearable electronics. With an idea to build a fiber-based battery, polymeric wires with enhanced ionic conductivity, and polymeric piezoactuators, we chose polyethlylene oxide (PEO)-PVDF blend as a precursor material for nanofiber yarns. PVDF is known for its chemical inertness and stability due to the presence of $-CF_2$ groups. Also, it is attractive polymer because of to its ferroelectric properties (2). PEO is widely used as an immobile solvent for metal ions in batteries (3).

2 EXPERIMENTAL

The nanofibers were produced by electrospinning method (Figure 1). The main advantage of this top-down electrospinning nanomanufacturing technology is relatively low cost compared to the synthetic bottom-up methods (4, 5).

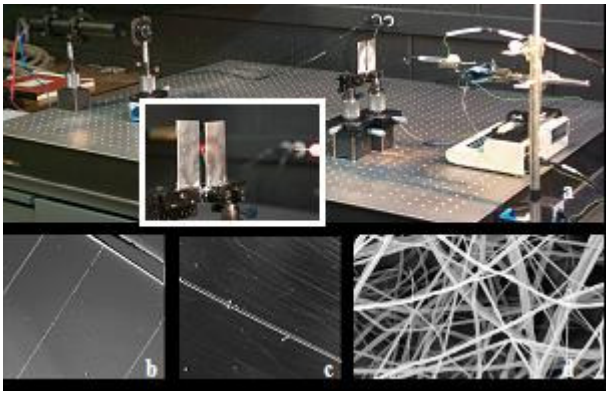

Figure 1: a) Electrospinning set up for production of linear assemblies of aligned nanofibers based on the gap method (6). b)-c) Examples of highly aligned and spaced linear assemblies of nanofibers, the diameter of the reference wire is 70 μm. d) Typical nonwoven material produced from nanofibers.

MATERIALS

Dimethylacetamide (DMA) and PEO (M_W=1,000,000) were obtained from Sigma-Aldrich. PVDF was purchased from Goodfellow.

ELECTROSPINNING DESIGN (ESD) SETUP

10-mL syringe with polymer solution (0.2 g of PEO and 2 g of PVDF in 10 g of DMA) covered with heater (55 ^oC) was attached to a syringe-type infusion pump. A stainless-steel needle of the syringe was connected to high-voltage and the system was grounded to a collector (Figure 1). Distance between two collectors, flow rate of polymer solution and temperature were constant. Voltage was the only variable in the experiments.

CHARACTERIZATIONS

The PVDF/PEO nanofibers were sputtered with platinum and examined using FESEM-Hitachi 4800 scanning electron microscopy (SEM).

Melting point and crystallinity of PVDF/PEO blend were determined by differential scanning calorimety (DSC-2920, TA Instruments). For DSC two runs were performed. The first run (from -100 ^oC to 120 ^oC at 10 $^oCmin^{-1}$) was carried out to eliminate the solvent. The second run (from -100 ^oC to 250 ^oC at 20 $^oCmin^{-1}$) was used to calculate the degree of fibers' crystallinity. The enthalpy of melting for pure PEO (7) and PVDF (8) was used to calculate the crystallinity.

Thermal gravimetric analysis (Hi-Res TGA-2950, TA Instruments) allows one to determine decomposition temperature of PVDF and PEO in nanofibers.

Fourier transform infrared spectroscopy (FTIR) (Magna-IR spectrometer 550, Nicolet) was used to detect the presence of β-phase.

3 RESULT AND DISCUSSION

The yarns produced from PVDF/PEO nanofibers (Figure 2a) have higher tenacity compare to the ones formed from pristine PVDF. SEM image (Figure 2b) indicates that the fibers have average diameter around 1.2 μm and are highly porous.

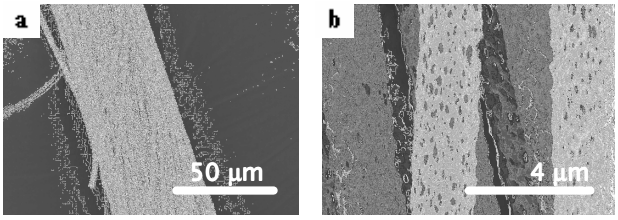

Figure 2: a) Yarn produced from b) PVDF/PEO nanofibers.

Wettability

The surface chemical structure of our fibers was analyzed using wetting experiments. It appears that water droplet deposited on the yarn surface does not penetrate the yarn (Figure 4a). In experiments with nanofiber yarn made of pristine PEO, water droplet broke the yarn almost immediately after touching it. On PVDF/PEO yarns, water droplet forms a clamshell-like configuration, while ethylene glycol droplet takes a barrel-like configuration (Figure 3b)

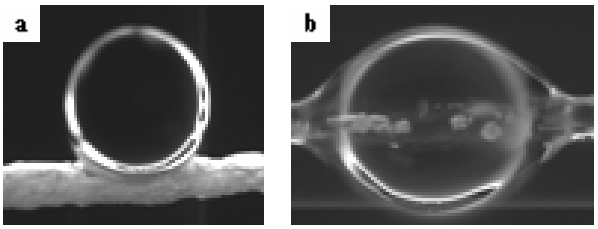

Figure 3: (a) Water and (b) ethylene glycol droplets on the yarn

penetrates inside eventually.

We assume that the fibers have a core-skin structure with a core made of PEO and a skin made of PVDF (Figure 4).

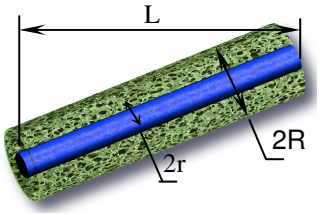

Figure 4: Schematic picture of a core-skin fiber.

Core radius of PVDF/PEO fiber was calculated using equation 1 and is equal to 440 nm.

$$\frac{V_{PEO}}{V_{PVDF}} = \frac{\pi r^2 L}{\pi R^2 L - \pi r^2 L} = \frac{M_{PEO}}{(M_{PEO}+M_{PVDF})\rho_{PEO}} \Big/ \frac{M_{PVDF}}{(M_{PEO}+M_{PVDF})\rho} \quad (1)$$

where, M-is the weight of particular polymer, ρ-its density

The PVDF-air interfacial tension is lower (30 mN/m) than that of PEO in air (42.9 mN/m) (http://www.surface-tension.de/solid-surface-energy.htm). Therefore, it seems reasonable to assume that PEO forms a core in order to minimize its surface free energy. Moreover, in our experiments, PEO had much higher molecular weight and precipitates first. Being wet by DMA/PVDF solution, the PEO nuclei, most likely, become displaced from the jet surface. Precipitation of PVDF, thus, occurs at the PEO surface. When DMA protrudes through the PVDF precipitate it forms pores visible in Figure 2b.

Porosity

To determine the porosity of the nanofiber microsized piece of us spun fiber was cut using the tip of atomic force microscope (AFM) and was glued to it (Figure 5).

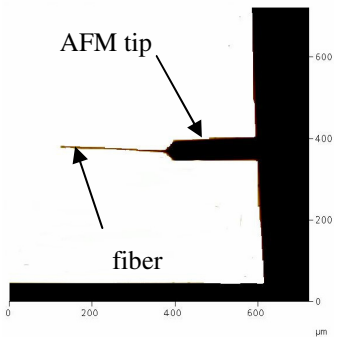

Figure 5: An optical image of the fiber attached to AFM tip

The fiber weight was determined by the change in the tip resonance frequency. Next, the fiber was immersed into Galwick (Porous Materials, Inc). Because Galwick has very low surface tension (16 dynes/cm^2) it wets PVDF surface, it fills the fiber pores. New value of the resonance frequency of the wet fiber-cantilever system was used to calculate the weight of wet fiber. Since, elastic constant of this complex spring is maintained the same the change of the frequency is, thus, controlled mostly by the added mass.

Fiber porosity was estimated using the volume of the Galwick that penetrated into pores. Assuming that all pores were filled completely with Galwick, the nanofiber porosity was estimated using equation 2 and found to be $\varepsilon =$ 0.82

NSTI-Nanotech 2008, www.nsti.org, ISBN 978-1-4200-8504-4 Vol. 2

$$\varepsilon = \frac{V_{galwic}}{V_{galwick} + V_{fiber}} \qquad (2)$$

$$V_{fiber} = \frac{M_{PEO}}{M_{PEO} + M_{PVDF}} \frac{M_{fiber}}{\rho_{PEO}} + \frac{M_{PVDF}}{M_{PEO} + M_{PVDF}} \frac{M_{fiber}}{\rho_{PVDF}}$$

where, $M_{galwick}/M_{fiber}$ = 5.12, $\rho_{galwick}$=1.8212 g/cm^3, ρ_{PVDF}=1.76 g/cm^3, ρ_{PEO}=1.13 g/cm^3

Crystal stucture

PVDF forms several types of crystals, which can provide distinct absorption signals in IR range. We compared the spectra of casted PVDF films and electrospun yarns formed at 7.5 kV (Figure 6).

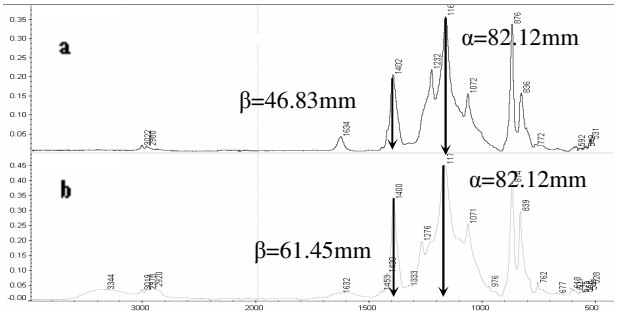

Figure 6: FTIR spectra of (a) cast PVDF film and (b) yarns electrospun at 7.5kV.

The ratio of the peak heights between β (1170 cm^{-1}) and α (1400 cm^{-1})-phases is higher for the electrospun fibers indicating the higher content of β-crystals in the fibers. Figure 7a shows the differences of the β/α ratios for PVDF pellets, cast films, and electrospun fibers. Ratio of β/α phase for electrospun fibers did not change in 5 days (Figure 7b).

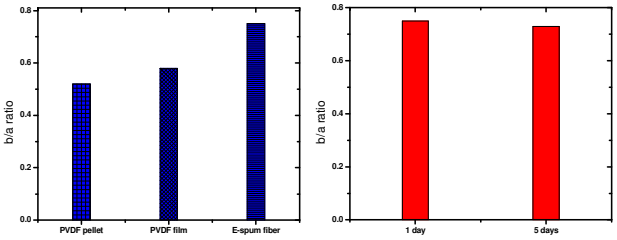

Figure 7: (a) β/α ratios for PVDF pellets, castled films, and electrospun fibers and (b) aging test for electrospun fibers

The height of the peak at 1400 cm^{-1} corresponding to β-phase (and, consequently, its content) depends on applied voltage (Figure 8). Maximum height is reached at 7.5 kV.

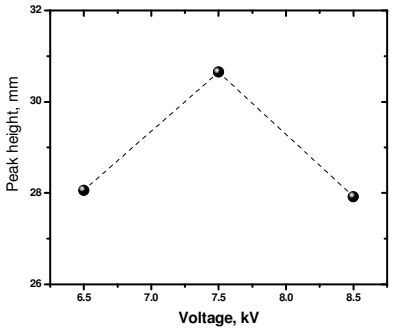

Figure 8: Correlation between peak height of β-phase (1400 cm^{-1}) and spinning voltage

The results of TGA measurements for freshly prepared fibers are presented in Figure 9. They suggest that the fiber can initially contain some amount of solvent (about 4 %). The decomposition temperature of PEO and RNDF were found to be 367^{0}C and 433^{0}C, respectively.

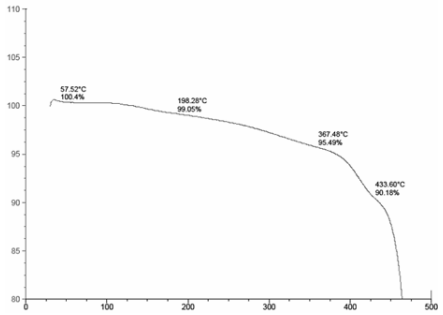

Figure 9: TGA curve of PEO/PVDF fibers.

DSC analysis of PVDF/PEO nanofibers was performed using the algorithm motioned in the Experimental part. It can be noticed that the intensity of the endothermic peak at 60^{0}C that corresponds to PEO crystals dramatically decreases after second run (Figure 10).

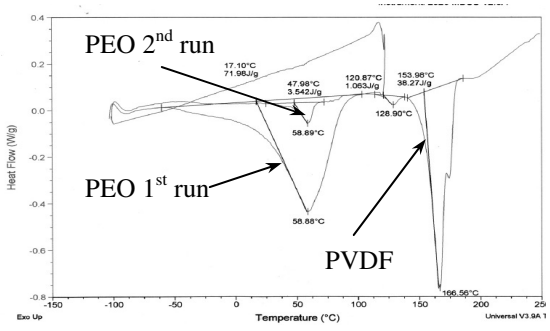

Figure 10: DSC analysis of PVDF/PEO fibers without water treatment

Calculated degree of crystallinity of PEO and PVDF were 1.7% and 36%, respectively.

CONCLUSIONS

We showed that yarns from PVDF/PEO nanofibers electrospun from DMA solutions form highly porous materials, with ~ 82% porosity, these yarns offer many opportunities as probing materials. DSC and FTRI analysis suggest that the $\beta-$crystallinity in these materials is high ~ 36%. The yarns seem to have core-shell structure with the skin made of hydrophobic PVDF and the core made of hydrophilic PEO. Preliminary results show that the yarns can be irreversibly bent by applying electric field.

Acknowledgement.

We acknowledge the support from Department of Commerce through National Textile Center (Grant # M08-CL10). We appreciate continuous help of K.Ivey, O.Hoy and B.Zdyrko.

REFERENCES

[1] N.V. Bhat,. D.T. Seshadri, S. Radhakrishnan, Text. Res. J., 74, 155, 2004.

[2] R.G. Kepler, in Ferroelectric Polymers: Chemistry, Physics, and Applications, H.S. Nalwa, Ed., Marcel Dekker, New York, 183, 1995.

[3] M. S. Michael, M. M. Jacob, E. Prabaharan, R. S. Radhakrishna, Solid State Ionics, 98, 167,1997.

[4] D.H. RenekerYarin, A.L Zussman, E. Xu, Adv. Appl. Mech., 41, 44, 2006.

[5] W.E. Teo, S. Ramakrishna, Nanotechnology, 17, R89, 2006.

[6] D. Li, Y.L. Wang, Y.N. Xia, Nano Lett., 3, 1167, 2003.

[7] Polymer Data Handbook,. J.E. Mark, Ed., Ox. Univ. Press, N.Y. 1999.

[8] Y. Rosemberg, A. Sigmann, M. Narkis, S. Shkolnik, J. Appl. Polym. Sci., 43, 535, 1991.